



UNIVERSITY  
OF WOLLONGONG  
AUSTRALIA

University of Wollongong  
Research Online

---

Australian Institute for Innovative Materials - Papers

Australian Institute for Innovative Materials

---

2016

# Synthesis and characterization of covalently linked graphene/chitosan composites

Sepidar Sayyar

*University of Wollongong, [sepidar@uow.edu.au](mailto:sepidar@uow.edu.au)*

Eoin Murray

*University of Wollongong, [eoin@uow.edu.au](mailto:eoin@uow.edu.au)*

Sanjeev Gambhir

*University of Wollongong, [sanjeev@uow.edu.au](mailto:sanjeev@uow.edu.au)*

Geoffrey M. Spinks

*University of Wollongong, [gspinks@uow.edu.au](mailto:gspinks@uow.edu.au)*

Gordon G. Wallace

*University of Wollongong, [gwallace@uow.edu.au](mailto:gwallace@uow.edu.au)*

*See next page for additional authors*

---

## Publication Details

Sayyar, S., Murray, E., Gambhir, S., Spinks, G., Wallace, G. G. & Officer, D. L. (2016). Synthesis and characterization of covalently linked graphene/chitosan composites. *JOM*, 68 (1), 384-390.

Research Online is the open access institutional repository for the University of Wollongong. For further information contact the UOW Library:  
[research-pubs@uow.edu.au](mailto:research-pubs@uow.edu.au)

---

# Synthesis and characterization of covalently linked graphene/chitosan composites

## **Abstract**

Chitosan, a naturally derived polysaccharide, was covalently linked to chemically converted graphene (CCG) and the properties of the resulting composites were investigated. The composites were prepared using a stable dispersion of CCG in aqueous solvent. The CCG sheets are stabilised in solution by a small number of peripheral charged groups that can be used to form amide linkages with the polymer matrix. Apart from processability and swellability, the synthesized composites exhibited improved mechanical properties and conductivity by the addition of graphene. Graphene incorporation also introduced a control over the extent of swelling in the composites. The synthesized graphene/composites are promising materials for a variety of applications, for example as conducting substrates for the electrically stimulated growth of cells.

## **Keywords**

covalently linked, characterization, chitosan, composites, synthesis, graphene

## **Publication Details**

Sayyar, S., Murray, E., Gambhir, S., Spinks, G., Wallace, G. G. & Officer, D. L. (2016). Synthesis and characterization of covalently linked graphene/chitosan composites. *JOM*, 68 (1), 384-390.

## **Authors**

Sepidar Sayyar, Eoin Murray, Sanjeev Gambhir, Geoffrey M. Spinks, Gordon G. Wallace, and David L. Officer

# Synthesis and Characterization of Covalently Linked Graphene/Chitosan Composites

S. SAYYAR,<sup>1</sup> E. MURRAY,<sup>1,2</sup> S. GAMBHIR,<sup>1</sup> G. SPINKS,<sup>1</sup> G.G. WALLACE,<sup>1</sup>  
and D.L. OFFICER<sup>1,3</sup>

1.—ARC Centre of Excellence for Electromaterials Science (ACES), Intelligent Polymer Research Institute, AIIM Facility, Innovation Campus, University of Wollongong, Wollongong, NSW 2522, Australia. 2.—e-mail: murray@ntu.edu.sg. 3.—e-mail: davidoff@uow.edu.au

Chitosan, a naturally derived polysaccharide, was covalently linked to chemically converted graphene (CCG) and the properties of the resulting composites were investigated. The composites were prepared using a stable dispersion of CCG in aqueous solvent. The CCG sheets are stabilised in solution by a small number of peripheral charged groups that can be used to form amide linkages with the polymer matrix. Apart from processability and swellability, the synthesized composites exhibited improved mechanical properties and conductivity by the addition of graphene. Graphene incorporation also introduced a control over the extent of swelling in the composites. The synthesized graphene/composites are promising materials for a variety of applications, for example as conducting substrates for the electrically stimulated growth of cells.

## INTRODUCTION

The development of suitable materials for biomedical applications, especially tissue engineering, has been the focus of much recent materials research.<sup>1,2</sup> The ideal tissue engineering material should be biocompatible and processable with the appropriate mechanical properties for cell and tissue development and support.<sup>3</sup> In addition, it has recently been shown that electrically conducting substrates can induce and direct improved cell growth of electro-responsive cells under electrical stimulation.<sup>4–6</sup>

Chitosan, a semi-crystalline natural polymer derived from chitin, is a promising material for the development of biomaterials. Due to its good biocompatibility and biodegradability, chitosan has been used in a large number of applications such as artificial skin, tissue engineering and drug delivery.<sup>7</sup> Furthermore, the good swelling behaviour of chitosan makes it an appropriate candidate to form hydrogels for tissue engineering scaffolds.<sup>8–11</sup>

It has been shown that the inherent properties of the natural polymers can be modified or even improved by the incorporation of carbonaceous fillers resulting in a range of materials suitable for a wide variety of applications.<sup>12–16</sup> Graphene, a

planar monolayer of carbon material arranged in a honeycomb lattice with excellent mechanical, electrical and thermal properties, has been shown to be an excellent material with which to modify biopolymers for tissue engineering without affecting their biocompatibility or processability.<sup>17–23</sup> The advantage of graphene over the other carbonaceous fillers, e.g. carbon nanotubes, is its facile and inexpensive synthesis and its potential for scaled-up manufacturing in solution form.<sup>24</sup>

Here, we report the preparation of covalently linked graphene/chitosan composites using lactic acid as a solubilising agent. The cross-linking and resulting physical properties of the composites have been characterized and compared to similarly cross-linked chitosan without graphene fillers.

## MATERIALS AND METHODS

### Materials

Chitosan powder (medium molecular weight), P<sub>2</sub>O<sub>5</sub>, 1-ethyl-3-(3-dimethylaminopropyl)carbodiimide hydrochloride (EDC) and *N*-hydroxysuccinimide (NHS) were sourced from Sigma-Aldrich. DL-lactic acid (80–85% aqueous solution) was purchased from Alfa Aesar. Graphite powder was obtained from Bay Carbon. Sulphuric acid and 30% H<sub>2</sub>O<sub>2</sub> were

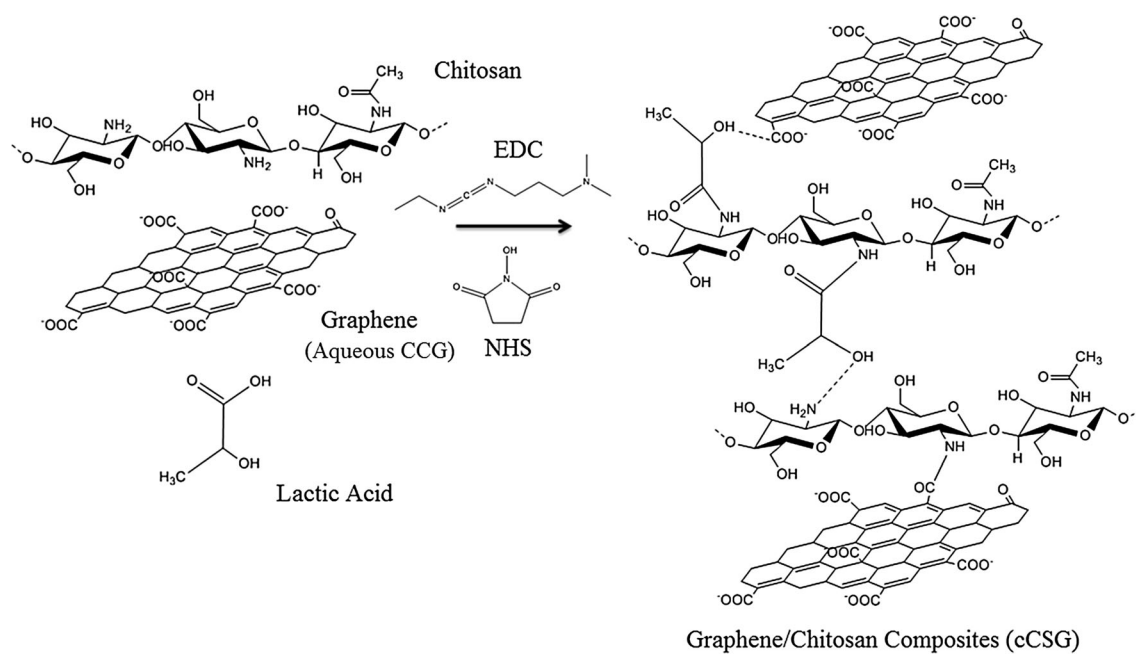


Fig. 1. Preparation of graphene/chitosan composites by covalent attachment.

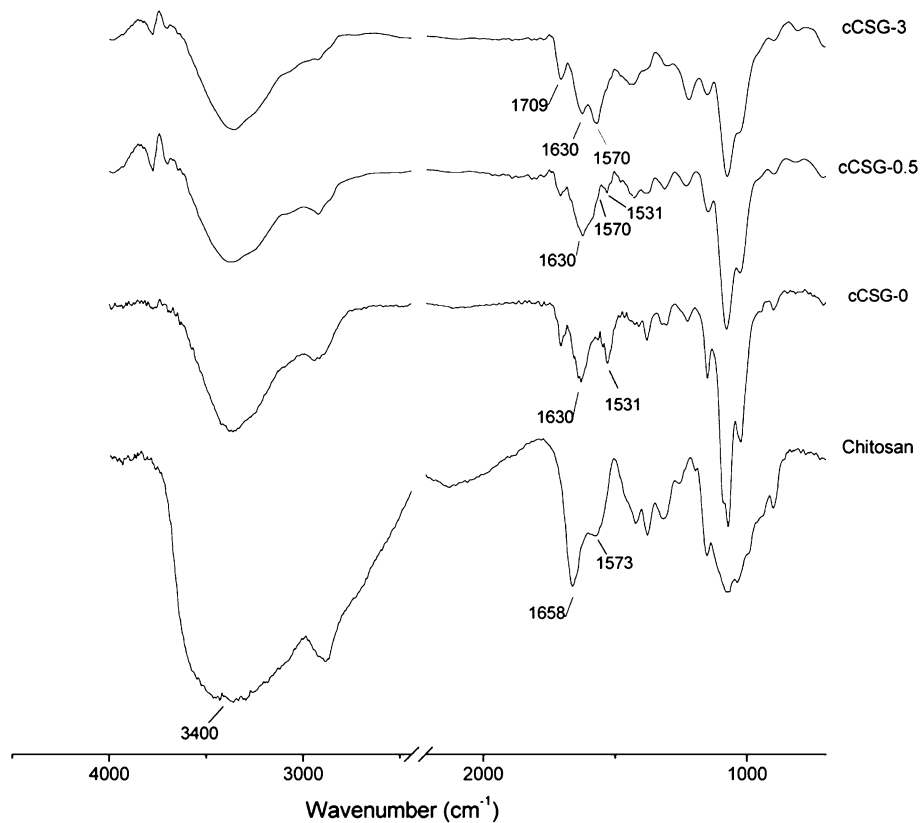


Fig. 2. FTIR spectra of chitosan and cCSG samples with different graphene content.

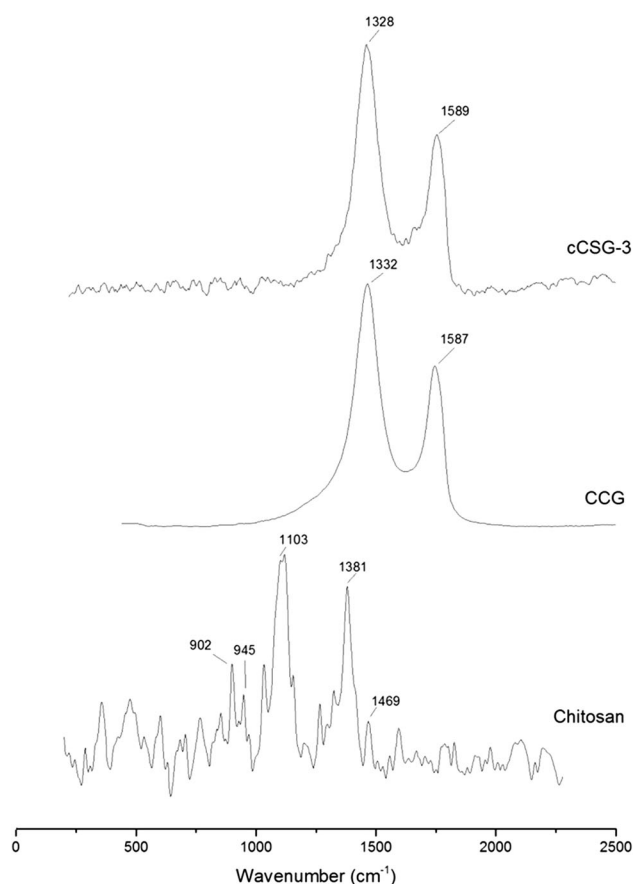


Fig. 3. Raman spectra of chitosan, CCG and the composite containing 3 wt.% graphene (cCSG-3).

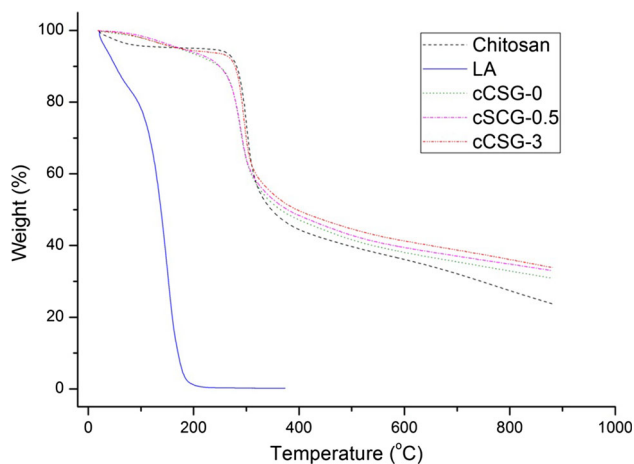


Fig. 4. Thermogravimetric curves of pristine chitosan, lactic acid (LA) and cCSG samples prepared with 0 wt.%, 0.5 wt.% and 3 wt.% graphene, respectively.

purchased from Ajax Finechem.  $K_2S_2O_8$  and  $KMnO_4$  were obtained from Chem-supply. Milli-Q water with a resistivity of  $18.2 \text{ m}\Omega \text{ cm}^{-1}$  was used in all preparations.

## Preparation of Chemically Converted Graphene Oxide Dispersion

Graphene oxide (GO) was synthesised from natural graphite powder using a modified Hummers' method.<sup>25,26</sup> The reduction was carried out in two steps to achieve better oxidation of graphite.<sup>26</sup> In the first step, the graphite was pre-oxidised using  $K_2S_2O_8$ ,  $P_2O_5$  and  $H_2SO_4$ , followed by  $H_2SO_4$ ,  $KMnO_4$  and  $H_2O_2$  in the second step. The synthesised GO was then exfoliated in water by sonication to give a 0.05 wt.% aqueous GO dispersion. The resultant GO dispersion was chemically converted to graphene (CCG) using hydrazine and ammonia at  $95^\circ\text{C}$  under stirring for 1 h. The resulting aqueous dispersion with a graphene concentration of  $0.5 \text{ mg ml}^{-1}$  was stable for several weeks. It has previously been shown that the materials developed using this CCG are biocompatible and appropriate for cell culture.<sup>20,21,23,27</sup>

## Preparation of Covalently Linked Chitosan Composites

To prepare covalently linked chitosan samples (cCSG), chitosan powder (2% w/v) was added to deionised (DI) water or required volume of aqueous CCG followed by slow addition of lactic acid (with a 2:1 w/w ratio relative to chitosan) under stirring. The solution was then sonicated for 20 min. Then, NHS (0.2% w/v) was added and the solution was stirred for 30 min followed by addition of EDC (0.5% w/v). After stirring for 3 h and mild sonication, the mixture was poured into a Petri dish to evaporate the water and dried at  $50^\circ\text{C}$ . The samples were labelled cCSG-0, cCSG-0.1, cCSG-0.5, cCSG-1.5 and cCSG-3, according to the weight percentage of the graphene content per chitosan, with cCSG-0 containing no graphene and cCSG-3 containing 3 wt.%.

## CHARACTERIZATION METHODS

For all testing in the dried state, the materials used were dried thoroughly and kept in a desiccator until analysis. FTIR spectra were taken on a Shimadzu IRPrestige-21 infrared spectrometer in the range from  $400 \text{ cm}^{-1}$  to  $4000 \text{ cm}^{-1}$ . Raman spectra were recorded on a Jobin Yvon Horiba HR800 Raman microscope using a 632-nm laser line and a 300-line grating. The morphology of the films was observed using a field-emission SEM instrument (JEOL JSM-7500FA). Samples were frozen in liquid nitrogen, fractured and sputter-coated (EDWARDS Auto 306) with a thin layer of gold ( $\approx 12 \text{ nm}$  thickness). Thermogravimetric analyses (TGA) was carried out using a TA Instruments TGA Q500 with a heating rate of  $10^\circ\text{C}$  under nitrogen atmosphere. All sonication was done using a Branson Digital Sonicator (S450D, 500 W, 40% amplitude). The mechanical properties were measured using an

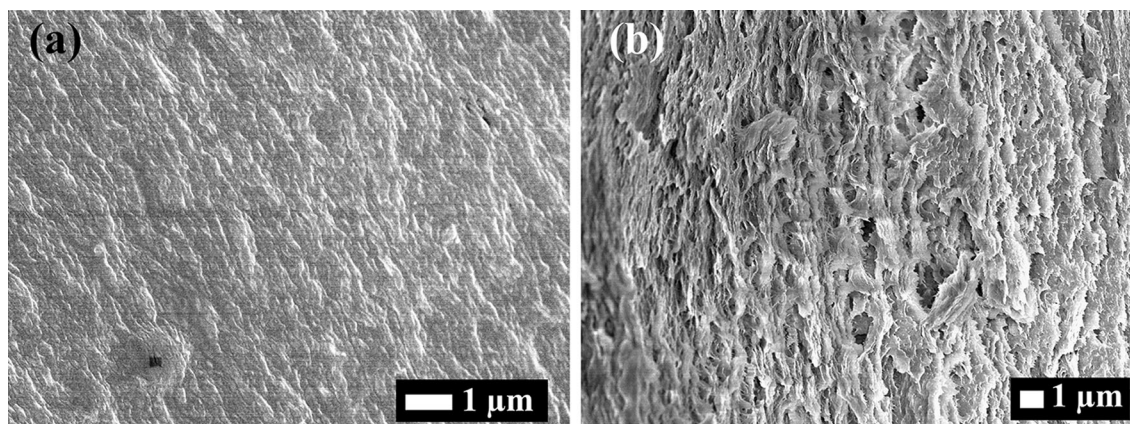


Fig. 5. SEM images of the surface (a) and cross section (b) of the cCSG-3 film.

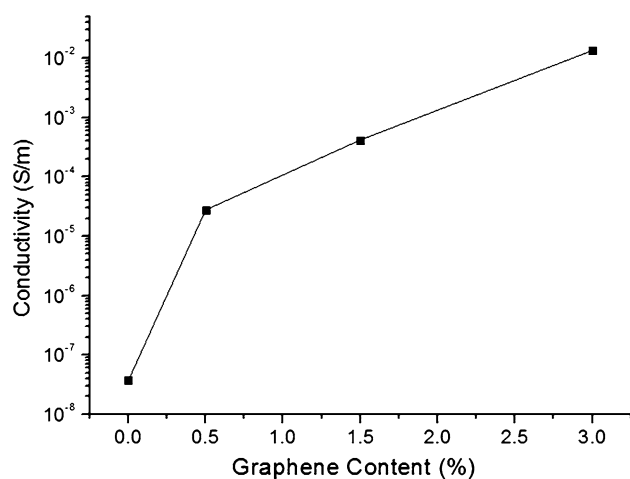


Fig. 6. Conductivity measurements of cCSG films with different graphene contents.

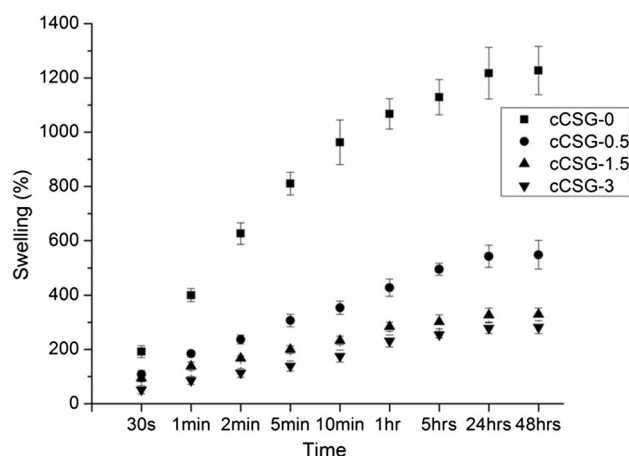


Fig. 7. Swelling characteristics of cCSG films with different graphene contents in DI water over 48 h.

Instron 5566 Universal Testing Machine (USA) at a constant rate of  $5 \text{ mm min}^{-1}$ . The samples were cut into strips with a width of 3 mm and a length of 20 mm. The electrical conductivity of the composite films was measured using a four-point probe resistivity measurement system (JG 293015 Jandel) at room temperature. All the conductivity values are the average of five consecutive measurements. The swelling properties were measured through placing a known weight of the samples in DI water. At different time intervals, the samples were removed from the water, patted dry with a wiper and immediately weighed on an electronic balance at room temperature. The percentage swelling of the composite in the water were then calculated from the formula:

$$E_{sr} = [(W_s - W_d) / W_d] \times 100 \quad (1)$$

where  $E_{sr}$  is the percent swelling of the sample (%),  $W_s$  denotes the weight of the sample in swollen state and  $W_d$  is the initial weight of the sample.

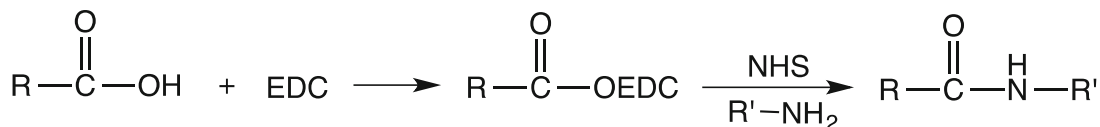
## RESULTS AND DISCUSSIONS

The feasibility of developing covalently linked graphene/chitosan composites was investigated in this study. In previous work,<sup>20</sup> we showed that covalently linking graphene to elastomeric polymer chains resulted in better dispersion of graphene nanosheets inside the polymer matrix and improvements in the mechanical and electrical properties.

Acetic acid is the most commonly used acid for solubilising and cross-linking the chitosan for the development of chitosan films. However, this acid can negatively affect cell growth.<sup>28</sup> Lactic acid has been shown to be a more appropriate cross-linker for the development of chitosan biocomposites due to its reduced cytotoxicity.<sup>28</sup> In addition, the hydroxyl and carboxyl functional groups can be utilised to link the polymer chains to the filler. The presence of carboxyl groups in graphene and lactic acid as well as amine groups in chitosan provides the opportunity for covalently linking these components



through the formation of amide groups using appropriate coupling agents such as 1-ethyl-3-(3-dimethylaminopropyl)carbodiimide (EDC) and NHS as shown in Eq. 2 and used to couple chitosan to carbon nanotubes:<sup>29,30</sup>



The samples were prepared through a facile solution-blending method using aqueous CCG, lactic acid and the coupling agents. The schematic of the reaction is shown in Fig. 1. The developed composites were characterized to study the effect of covalent attachment and addition of graphene on the polymer.

#### FOURIER TRANSFORM INFRARED SPECTROSCOPY

Fourier transform infrared spectroscopy (FTIR) can be an effective technique for assessing the interaction between the components of a

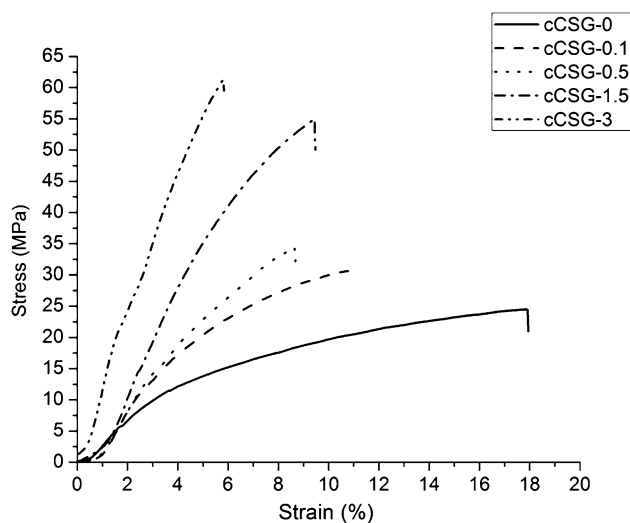


Fig. 8. Stress-strain curves of cCSG samples in the dry state.

composite. FTIR spectroscopy has the potential to identify the new amide linkages formed between the lactic acid, graphene and the chitosan. Figure 2 shows the FTIR spectra of chitosan and cCSG films.

The FTIR spectrum of chitosan shows the characteristic chitosan peaks. The strong absorbance bands at  $1658\text{ cm}^{-1}$  and  $1573\text{ cm}^{-1}$  correspond to the chitosan amide C=O stretching and amine N-H bending vibrations, respectively. The broad peak around  $3400\text{ cm}^{-1}$  is assigned to the amine N-H stretching vibrations. The absorption peaks between  $1037\text{ cm}^{-1}$  and  $1153\text{ cm}^{-1}$  are attributed to the primary amine and primary and secondary alcohol groups. The bands between  $2800\text{ cm}^{-1}$  and  $3000\text{ cm}^{-1}$  are characteristic of C-H stretches.<sup>16,31</sup>

In the covalently linked sample without graphene (cCSG-0), two new peaks appear at  $1630\text{ cm}^{-1}$  and  $1531\text{ cm}^{-1}$ . The peak at  $1630\text{ cm}^{-1}$  can be attributed to the C=O stretching of the secondary amide groups present in the newly formed covalent linkages between the amine groups of chitosan and the carboxyl groups of lactic acid. The other new peak at  $1531\text{ cm}^{-1}$  is proposed to be due largely to the N-H bending vibration of the new amide groups. There is also a significant drop in the intensity of the broad band at around  $3400\text{ cm}^{-1}$  presumably as a result of the reaction of the chitosan  $\text{NH}_2$  groups. On the addition of graphene, there is almost no change in the IR spectrum other than a clear decrease in the intensity of the peak at  $1531\text{ cm}^{-1}$  with a concomitant appearance of a new peak at  $1570\text{ cm}^{-1}$ . Given the increasing intensity of the  $1570\text{ cm}^{-1}$  with increasing amounts of graphene, it is likely that this band is due to new N-H bending vibrations arising from the covalent linkages between graphene and chitosan. The peak at  $1709\text{ cm}^{-1}$ , which is present in all the CSG spectra, results from non-bonded COOH groups of lactic acid, suggesting that not all the lactic acid is covalently bound. Thus, there are

Table I. Mechanical properties of cCSG samples with different graphene contents

Sample	Tensile strength (MPa)	Elongation at break (%)	Young's modulus (MPa)
cCSG-0	$24.4 \pm 1.2$	$17.8 \pm 0.6$	$462 \pm 23$
cCSG-0.1	$29.9 \pm 1.1$	$11.1 \pm 1.2$	$650 \pm 20$
cCSG-0.5	$34.5 \pm 1.5$	$8.7 \pm 0.7$	$691 \pm 24$
cCSG-1.5	$54.3 \pm 0.9$	$9.4 \pm 0.2$	$995 \pm 19$
cCSG-3	$61.4 \pm 1.8$	$5.8 \pm 0.7$	$1665 \pm 41$

clear changes in the FTIR spectra that appear to result from the covalent attachment of the graphene sheets to the lactate-substituted chitosan.

### RAMAN SPECTRA

Raman spectra of chitosan, CCG and the composite with 3 wt.% CCG content (cCCG-3) were obtained between  $400\text{ cm}^{-1}$  and  $2500\text{ cm}^{-1}$  (Fig. 3). The typical peaks of chitosan are evident with  $\text{NH}_2$  wagging at  $902\text{ cm}^{-1}$ , ether bonds and the stretching of glycosidic peaks around  $1103\text{ cm}^{-1}$ , and the methyl group bends around  $1381\text{ cm}^{-1}$ .<sup>32</sup> In the spectra of CCG and the composite cCCG-3, only the two peaks at  $1332\text{ cm}^{-1}$  and  $1587\text{ cm}^{-1}$  characteristic of the D and G bands of graphene are evident, supporting the presence of graphene in the composite cCCG-3; no chitosan peaks can be seen in the cCSG-3 sample due to the dominant nature of the graphene bands. The position of the bands and the  $I_D/I_G$  ratio (1.51 for CCG versus 1.59 for cCSG-3) is little changed in the composite, suggesting that there are few differences in the size and structure of the CCG nanosheets inside the matrix.<sup>23,33,34</sup>

### THERMOGRAVIMETRIC ANALYSIS

Thermogravimetric analyses (TGA) of chitosan, lactic acid and cCSG samples are shown in Fig. 4. The TGA of pristine chitosan shows a slight weight loss around  $100^\circ\text{C}$  that is due to the release of the moisture trapped in the chitosan matrix followed by the decomposition of the polymer structure around  $250^\circ\text{C}$ . Lactic acid (LA) shows two weight loss regions, one between  $25^\circ\text{C}$  and  $100^\circ\text{C}$  due to water evaporation, and the other between  $100^\circ\text{C}$  and  $200^\circ\text{C}$ , corresponding to the decomposition of the lactic acid structure.

The thermal decomposition of the cCSG composites occurs in three main stages starting with a slow weight loss between  $90^\circ\text{C}$  and  $250^\circ\text{C}$  that is attributed to water and lactic acid loss. Then, there is a major weight loss between  $250^\circ\text{C}$  and  $340^\circ\text{C}$  likely due to chitosan decomposition followed by a slow weight loss from  $340^\circ\text{C}$  to  $900^\circ\text{C}$ , corresponding to partial graphene decomposition. The covalent attachment of graphene has enhanced the thermal stability of the samples from around  $250^\circ\text{C}$  in the cCSG-0 to more than  $270^\circ\text{C}$  in the cCSG-3 composite. It is evident from the TGA curves of the cCSG samples that the excess amount of lactic acid is removed during the washing step. The residual carbon remaining due to graphene, after taking residual polymer into consideration, was found to be around 3 wt.% for the cCSG-3 sample, consistent with the percentage of graphene initially added to the reaction.

### SCANNING ELECTRON MICROSCOPY

Figure 5 shows scanning electron microscopy (SEM) images of the surface and cross-section of cCSG films with 3 wt.% graphene loadings. No

aggregation can be observed on the surface and cross-section of the films confirming that the graphene sheets are well dispersed throughout the chitosan matrix. The cross-sectional image of the cCSG-3 sample also shows a rough and dense inner structure in the composite matrix which is the result of the covalent attachment between the composite components.

### CONDUCTIVITY

The addition of graphene improved the electrical conductivity of the chitosan (Fig. 6). A conductivity of around  $1\text{E}-8\text{ S m}^{-1}$  for neat chitosan has been reported.<sup>35</sup> The conductivity of the cCSG sample is considerably increased to  $10\text{E}-5\text{ S m}^{-1}$  on addition of 0.5 wt.% graphene content. The conductivity keeps increasing on addition of graphene and reaches around  $1.4\text{E}-2\text{ S m}^{-1}$  in the cCSG composite with 3 wt.% CCG, corresponding to around 6 orders of magnitude improvement in the conductivity of the pristine chitosan.

### SWELLING STUDIES

Figure 7 shows the swelling properties of cCSG samples at different graphene contents. Generally, the samples swell at a constant rate that decreases after 24 h for all samples. cCSG-0 film swells quickly to more than 1000% in the first hour, followed by a slower swelling rate up to 1300% over 48 h. The swelling rate can be controlled by the addition of the hydrophobic graphene nanosheets. The swelling of cCSG composites was found to decrease with increasing graphene content with cCSG samples of 0.5 wt.%, 1.5 wt.% and 3 wt.% graphene contents swelling to 550%, 330% and 282%, respectively, after 48 h.

### MECHANICAL PROPERTIES

Typical stress-strain curves for cCSG films with different graphene concentrations are shown in Fig. 8 and the detailed data are summarised in Table I. These data show the effect on tensile strength and Young's modulus of the increasing addition of graphene in cCSG samples. With only 0.1 wt.% of graphene, a 22% improvement in tensile strength of cCSG films is observed. With 0.5 wt.% and 1.5 wt.% incorporation of graphene, the tensile strength values reached more than 34 MPa and 54 MPa, respectively. The tensile strength of the cCSG was further improved to more than 61 MPa on addition of 3 wt.% graphene, which is about 150% greater than the polymer alone (cCSG-0).

Similarly, the Young's modulus of cCSG films was also improved by the incorporation of graphene. The Young's modulus of cCSG-0 films was found to increase by more than 260% from 462 MPa to 1.7 GPa on addition of 3 wt.% graphene. The remarkable improvement in the tensile strength



and Young's modulus of the composites is attributed to homogeneous dispersion of graphene sheets inside the polymer matrix as well as the presence of strong covalent attachments between the graphene sheets and the polymer chains. However, as a result, the elongation at break of the samples decreases with increasing graphene content. This decrease is probably due to the covalent linkages between polymer and graphene restricting polymer chain movement.

## CONCLUSION

Graphene/chitosan composites were prepared by covalently linking graphene nanosheets to the polymer chains. A significant improvement in the thermal stability, tensile strength and modulus of the composite was observed with increasing graphene content. In addition, a six orders of magnitude improvement was observed over the conductivity of the polymer on addition of 3 wt.% graphene. Covalently linking graphene as a filler also allows control of the swelling rate of the polymer such that it can be accurately processed in controllable structures for implantation. As such, these covalently linked graphene/chitosan composites with enhanced mechanical and electrical properties are excellent candidates for use in structures for biomedical applications.

## ACKNOWLEDGEMENTS

This work was supported by the Australian Research Council (ARC) Super Science Fellowship scheme (FS100100023), the ARC Centre of Excellence Scheme (CE 140100012), the Australian Laureate Fellowship scheme (FL110100196) and the Australian National Fabrication Facility (ANFF). We also acknowledge use of the facilities and the assistance of Mr. Tony Romeo at the UOW Electron Microscopy Centre (EMC).

## REFERENCES

1. B. Guo, L. Glavas, and A.C. Albertsson, *Prog. Polym. Sci.* 38, 1263–1286 (2013).
2. M. Vert, *Biomacromolecules* 6, 538–546 (2004).
3. M.I. Sabir, X.X. Xu, and L. Li, *J. Mater. Sci.* 44, 5713–5724 (2009).
4. S. Jain, A. Sharma, and B. Basu, *Biomaterials* 34, 9252–9263 (2013).
5. S.Y. Park, J. Park, S.H. Sim, M.G. Sung, K.S. Kim, B.H. Hong, and S. Hong, *Adv. Mater.* 23, H263–H267 (2011).
6. C. Heo, J. Yoo, S. Lee, A. Jo, S. Jung, H. Yoo, Y.H. Lee, and M. Suh, *Biomaterials* 32, 19–27 (2011).
7. M. Rinaudo, *Prog. Polym. Sci.* 31, 603–632 (2006).
8. J.L. Drury and D.J. Mooney, *Biomaterials* 24, 4337–4351 (2003).
9. N. Bhattarai, J. Gunn, and M. Zhang, *Adv. Drug Deliv. Rev.* 62, 83–99 (2010).
10. J.K. Francis Suh and H.W.T. Matthew, *Biomaterials* 21, 2589–2598 (2000).
11. R. Riva, H. Ragelle, A. des Rieux, N. Duhem, C. Jerome, and V. Preat, *Adv. Polym. Sci.* 244, 19–44 (2011).
12. L. Hua, W. Kai, and Y. Inoue, *J. Appl. Polym. Sci.* 106, 1880–1884 (2007).
13. B. Das, K. Eswar Prasad, U. Ramamurty, and C.N. Rao, *Nanotechnology* 20, 125705 (2009).
14. X.M. Yang, L.A. Li, S.M. Shang, and X.M. Tao, *Polymer* 51, 3431–3435 (2010).
15. J.Z. Xu, T. Chen, C.L. Yang, Z.M. Li, Y.M. Mao, B.Q. Zeng, and B.S. Hsiao, *Macromolecules* 43, 5000–5008 (2010).
16. X.M. Yang, Y.F. Tu, L.A. Li, S.M. Shang, and X.M. Tao, *ACS Appl. Mater. Interfaces* 2, 1707–1713 (2010).
17. O. Yoon, I. Sohn, D. Kim, and N.-E. Lee, *Macromol. Res.* 20, 789–794 (2012).
18. W. Wang, Z. Wang, Y. Liu, N. Li, W. Wang, and J. Gao, *Mater. Res. Bull.* 47, 2245–2251 (2012).
19. X.Z. Tong, F. Song, M.Q. Li, X.L. Wang, I.J. Chin, and Y.Z. Wang, *Compos. Sci. Technol.* 88, 33–38 (2013).
20. S. Sayyar, E. Murray, B.C. Thompson, S. Gambhir, D.L. Officer, and G.G. Wallace, *Carbon* 52, 296–304 (2013).
21. S. Sayyar, R. Cornock, E. Murray, S. Beirne, D.L. Officer, and G.G. Wallace, *Mater. Sci. Forum* 773–774, 496–502 (2013).
22. E. Murray, B.C. Thompson, S. Sayyar, and G.G. Wallace, *Polym. Degrad. Stab.* 111, 71–77 (2015).
23. S. Sayyar, E. Murray, B.C. Thompson, J. Chung, D.L. Officer, S. Gambhir, G.M. Spinks, and G. Wallace, *J. Mater. Chem. B* 3, 481–490 (2015).
24. S. Gambhir, E. Murray, S. Sayyar, G.G. Wallace, and D.L. Officer, *Carbon* 76, 368–377 (2014).
25. W.S. Hummers and R.E. Offeman, *J. Am. Chem. Soc.* 80, 1339 (1958).
26. N.I. Kovtyukhova, P.J. Ollivier, B.R. Martin, T.E. Mallouk, S.A. Chizhik, E.V. Buzaneva, and A.D. Gorchinskiy, *Chem. Mater.* 11, 771–778 (1999).
27. H. Chen, M.B. Muller, K.J. Gilmore, G.G. Wallace, and D. Li, *Adv. Mater.* 20, 3557–3561 (2008).
28. S.E. Hismiogullari, A.A. Hismiogullari, F. Sahin, E.T. Oner, S. Yenice, and D. Karasartova, *J. Anim. Vet. Adv.* 7, 681–684 (2008).
29. R. Pauliukaite, M.E. Ghica, O. Fatibello-Filho, and C.M.A. Brett, *Anal. Chem.* 81, 5364–5372 (2009).
30. X.D. Cao, H. Dong, C.M. Li, and L.A. Lucia, *J. Appl. Polym. Sci.* 113, 466–472 (2009).
31. A. Pawlak and M. Mucha, *Thermochim. Acta* 396, 153–166 (2003).
32. C.E. Orrego, N. Salgado, J.S. Valencia, G.I. Giraldo, O.H. Giraldo, and C.A. Cardona, *Carbohydr. Polym.* 79, 9–16 (2010).
33. M.A. Pimenta, G. Dresselhaus, M.S. Dresselhaus, L.G. Cancado, A. Jorio, and R. Saito, *Phys. Chem. Chem. Phys.* 9, 1276–1291 (2007).
34. P. Hasin, M.A. Alpuche-Aviles, and Y. Wu, *J. Phys. Chem. C* 114, 15857–15861 (2010).
35. Y. Wan, K.A.M. Creber, B. Peppley, and V.T. Bui, *Macromol. Chem. Phys.* 204, 850–858 (2003).